Kobe University Repository : Kernel

PDF issue: 2026-11-14

CD11b+Gr－1dim Tolerogenic Dendritic Cell-Like Cells Are Expanded in Interstitial Lung Disease in SKG Mice

Sendo, Sho ; Saegusa, Jun ; Okano, Takaichi ; Takahashi, Soshi ; Akashi, Kengo ; Morinobu, Akio

(Citation)
Arthritis & Rheumatology,69(12):2314-2327

(Issue Date)
2017-12

(Resource Type)
journal article

(Version)
Accepted Manuscript

(URL)
https://hdl.handle.net/20.500.14094/90005883

KOBE UNIVERSITY

$CD11b^{+}Gr1^{dim}$ Tolerogenic Dendritic Cell-like Cells are Expanded in Interstitial Lung Disease in SKG Mice

Authors:

Sho Sendo MD,[1] Jun Saegusa MD.PhD,[1] Takaichi Okano MD.PhD,[1] Soshi Takahashi MD.PhD,[1] Kengo Akashi MD.PhD,[1] and Akio Morinobu MD.PhD[1]

Affiliation:

[1]Department of Rheumatology and Clinical Immunology, Kobe University Graduate School of Medicine, 7-5-2 Kusunoki-cho, Chuo-ku, Kobe 650-0017, Japan.

Please address correspondence and reprint request to:

Akio Morinobu, MD, PhD, Division of Rheumatology and Clinical Immunology, Department of Internal Medicine, Kobe University Graduate School of Medicine, 7-5-2, Kusunoki-cho, Chuo-ku, Kobe 650-0017, Japan

Phone: +81-78-382-6197; Fax: +81-78-382-6209

Email: morinobu@med.kobe-u.ac.jp

Running title:

$CD11b^{+}Gr1^{dim}$tolDC-like cells in ILD in SKG mice

This work was supported by Grant-in-Aid for Scientific Research from Japan Society for the Promotion of Science (16K09893). The authors declare no competing financial interests.

ABSTRACT

Objective. SKG mice develop interstitial lung disease (ILD) resembling rheumatoid arthritis-associated ILD (RA-ILD) in human. The aim of this study is to clarify the mechanism behind the lung pathology by analyzing the lung-infiltrating cells in ILD of SKG mice.

Methods. We assessed the severity of zymosan A (ZyA)-induced ILD in SKG mice histologically, and examined lung-infiltrating cells by flow cytometry. Total lung cells and isolated monocytic myeloid-derived suppressor cells (M-MDSCs) were cultured in vitro with GM-CSF (and IL-4). The proliferation of CSFE-labeled naïve T cells co-cultured with isolated $CD11b^{+}Gr1^{dim}$ cells and MDSCs was evaluated by flow cytometry. $CD11b^{+}Gr1^{dim}$ cells were transferred to ZyA-treated SKG mice.

Results. MDSCs, Th17 cells, and group 1 and 3 innate lymphoid cells (ILC1s and ILC3s) were increased in the lungs; the proportion of these cells varied with ILD severity. In this process, we found that a unique cell population, $CD11b^{+}Gr1^{dim}$ cells, were expanded in the severely inflamed lungs. About half of the $CD11b^{+}Gr1^{dim}$ cells expressed CD11c. The $CD11b^{+}Gr1^{dim}$ cells were induced from M-MDSCs with GM-CSF in vitro and were considered tolerogenic because they suppressed T-cell proliferation. The $CD11b^{+}Gr1^{dim}$ cells have never described previously and termed $CD11b^{+}Gr1^{dim}$ tolerogenic dendritic cell-like cells ($CD11b^{+}Gr1^{dim}$tolDC-LCs). Th17 cells, ILC1s and ILC3s in the inflamed lung produced GM-CSF, which may expand $CD11b^{+}Gr1^{dim}$tolDC-LCs in vivo. Furthermore, adoptive transfer of $CD11b^{+}Gr1^{dim}$tolDC-LCs significantly suppressed the progression of ILD in SKG mice.

Conclusion. We identified a unique suppressive myeloid cells termed CD11b^{+}Gr1^{dim}tolDC-LCs, which were differentiated from M-MDSCs, in ILD of SKG mice.

Introduction

Interstitial lung disease (ILD) is frequently complicated by connective tissue diseases (CTD), which are systemic autoimmune disorders of unknown origin. CTD-associated ILD is sometimes life-threatening, and it is important to elucidate its pathogenesis. ILD complicated by rheumatoid arthritis, a representative CTD, is called rheumatoid arthritis–associated ILD (RA-ILD). Both CD4^{+} T cells (1,2) and dendritic cells (DCs) (3) are significantly increased in RA-ILD compared to idiopathic ILD, suggesting that lymphoid and myeloid cells contribute to the pathogenesis of RA-ILD. Although some patients with RA-ILD respond to immunosuppressive therapy (4-6), others do not. Corticosteroids and other immunosuppressive therapies also have many side effects, including infection, making it desirable to find treatments with fewer side effects.

In SKG mice, which provide an animal model of rheumatoid arthritis, a single injection of zymosan A (ZyA) can induce not only arthritis but also ILD. These manifestations are due to a spontaneous point mutation of the gene encoding an SH2 domain of ZAP-70, which is a key transduction molecule in T cells. This ZAP-70 mutation leads to the thymic generation of autoimmune T cells, chronic arthritis, and extra-articular manifestations similar to rheumatoid arthritis (7,8).

DCs are potent antigen-presenting cells that can activate naïve T cells and

initiate adaptive immune responses. In general, DCs are derived from common DC progenitors and constitutively express CD11c on the cell surface (9). Several types of DCs with negative suppressive function have been reported as tolerogenic DCs (tolDCs), which are major regulators of immune responses in cancer, infection, autoimmune diseases, and transplantation (10-13). TolDCs suppress autoreactive T cells in the thymus during central tolerance, and limit effector T cells and promote regulatory T cell differentiation in the periphery. Previous reports describe roles of tolDCs in the intestine, lung, skin, liver, and other organs (14-18). Researchers have identified a tolDC subset in patients with chronic obstructive pulmonary disease (COPD) (19), and have demonstrated that the adoptive transfer of splenic tolDCs from helminth-infected mice can inhibit allergic inflammation in asthma-model mice (20). However, little is known about the role of tolDCs in RA-ILD. TolDCs can be generated from bone-marrow cells in vitro using GM-CSF and factors such as IL-10 and TGF-β (21,22); however, whether tolDCs can also be differentiated from lung-infiltrating cells is unknown.

Myeloid-derived suppressor cells (MDSCs), a heterogeneous cell population with immunosuppressive activities, are phenotypically defined as $CD11b^{+}Gr1^{+}$ cells and classified into two subpopulations: polymorphonuclear (PMN)-MDSCs with a $CD11b^{+}Ly6G^{+}Ly6^{low}$ phenotype, and monocytic (M)-MDSCs with a $CD11b^{+}Ly6G^{-}Ly6C^{high}$ phenotype (23). Although both tolDCs and MDSCs are tolerogenic and induced by GM-CSF, they differ in morphology, phenotype, and function. Some reports have identified tolDCs and MDSCs as potential therapeutic targets for inflammatory diseases (20,24,25), and others

have demonstrated the efficacy of intra-articular tolDC therapy for rheumatoid arthritis (26).

In this study, we found that the proportion of MDSCs was elevated in the lungs of ZyA-treated SKG mice, and detected a new population of $CD11b^{+}Gr1^{dim}$ cells. GM-CSF stimulation induced $CD11b^{+}Gr1^{dim}$ cells with tolDC-like characteristics from M-MDSCs. GM-CSF was produced by both helper T (Th) cells and innate lymphoid cells (ILCs). Furthermore, adoptive transfer of $CD11b^{+}Gr1^{dim}$tolDC-LCs significantly suppressed the progression of ILD in SKG mice. These results suggested that MDSCs could differentiate into $CD11b^{+}Gr1^{dim}$tolDC-LCs that served as the suppressor of ILD in SKG mice.

MATERIALS AND METHODS

Mice. Male SKG mice (CLEA Japan) were used at 3–20 weeks of age. All mice were kept in specific pathogen-free conditions at the Institute of Laboratory Animals, Graduate School of Medicine, Kobe University. All mice were handled in accordance with the guidelines for animal care approved by the Animal Experimentation Committee of Kobe University.

Reagents and antibodies. Zymosan A (ZyA) and 2-mercaptoethanol (2-ME) were purchased from Sigma-Aldrich; tofacitinib from Selleck Chemicals; DMSO from TOCRIS Bioscience; the carboxyfluorescein diacetate succinimidyl ester (CFSE-DA) Cell Proliferation Kit from Invitrogen; RPMI 1640 Medium and DMSO from Wako Pure Chemical Industries; fetal bovine serum (FBS) from MP Biomedicals; 1% penicillin-streptomycin from Lonza Walkersville; Liberase TL research grade from Roche; GM-CSF from Pepro Tech; and recombinant

mouse interleukin-4 (IL-4) protein, anti-TGF-β1, -β2, and -β3 antibody and mouse TGF-β1 ELISA Kit from R & D Systems. FITC-conjugated anti-Gr1 (FITC-anti-Gr1), PE-anti-Gr1 (Ly6G and Ly6C), FITC-anti-rat IgG2b k isotype, PE-anti-mouse isotype, purified hamster anti-mouse CD3e, purified hamster anti-mouse CD28, and purified rat anti-mouse CD16/CD32 (Fc block) were obtained from BD Biosciences. Brefeldin A, APC-anti-CD11b, PE-anti-CD11c, PE-anti-CD80, PE-anti-CD274 (PD-L1), FITC-anti-CD4, APC-anti-CD4, PE-anti-CD62L, PE-anti-CD80, PE-Cyanine7-anti-CD90.2 (Thy1.2), PE-anti-GM-CSF, PE-anti-FoxP3, PE-anti-RORγt, PE-anti-T-bet, APC-anti-RORγt, APC-anti-T-bet, PE-anti-ratIgG1 k isotype, APC-anti-IgG2a k isotype, and PE-Cyanine7-anti-ratIgG2a k isotype were obtained from eBioscience. Cell-staining buffer, nuclear-factor fixation and permeabilization buffer, FITC-anti-lineage cocktail (CD3/Gr1/CD11b/CD45R(B220)/Ter-119), FITC-anti-Ly6C, APC-anti-GATA3, and FITC-anti-hamster IgG/rat IgG2b/IgG2a were obtained from BioLegend.

Induction of arthritis and ILD in SKG mice. Male mice aged 8–9 weeks were given i.p. injections (5 mg) of ZyA (Sigma-Aldrich) suspended in 0.5 mg normal saline (SAL) as previously described (27) or SAL alone as a control.

Evaluation of arthritis. We assessed the development and severity of arthritis using a previously described system for scoring clinical arthritis (7). The scores for wrists and ankles and for all fingers of the fore and hind paws were totaled for each mouse. The maximum possible clinical arthritis score was 5.8.

Lung histology and scoring. The left lung was inflated with 4%

paraformaldehyde, embedded in paraffin, and sectioned by cryostat. The sections were stained with hematoxylin and eosin (H&E) and Masson's trichrome. All images were captured using a Keyence BZ-X710, and the images were combined to make the entire lung shape. The percentage of the affected area was calculated by Image J software (Wayne Rasband) as follows: {consolidation area + (cell infiltration without consolidation area) / 2} / whole lung area. The severity of ILD was evaluated by measuring the diffusely affected area as previously described (28), and assigning a histological score (HS); HS0 (normal), HS1 (10–30% affected), HS2 (30–60%), or HS3 (more than 60%).

Collection of bone marrow, spleen, and lung-infiltrating cells. Mice were euthanized with a high dose of pentobarbital sodium. The lungs were perfused with PBS via the trachea and right atrium to remove bronchoalveolar and blood cells. The right lung was incubated in RPMI1640, FBS, and Liberase TL (collagenase I and II) (Roche) for 45 min at 37 °C. The digested lungs were filtered through a 100-μm nylon filter and the cells collected. BM and spleen cells were directly filtered through a 100-μm nylon filter and collected.

Isolation of lung CD11b^{+}Gr1^{dim}tolDC-LCs, MDSCs, M-MDSCs, BM MDSCs, BM-derived DCs (BMDCs), and spleen naïve T cells. A BD FACSAria III (BD Biosciences) was used to sort CD11b^{+}Gr1^{dim}tolDC-LCs (CD11b^{+}Gr1^{dim} cells), MDSCs (CD11b^{+}Gr1^{+} cells), and M-MDSCs (CD11b^{+}Ly6C^{high} cells) from the lung, MDSCs and BMDCs from bone marrow, and naïve T cells (CD4^{+}CD62L^{+} cells) from the spleen.

Cell staining and flow cytometry. For surface staining, single-cell

suspensions of lung cells, bone-marrow cells, and splenocytes were washed with cell-staining buffer (BioLegend) and stained with anti-Gr1, anti-Ly6C, anti-CD11b, anti-CD11c, anti-CD80, anti-PD-L1, anti-CD4, anti-CD62L, anti-CD90.2, and anti-cocktail antibodies for 30 min at 4 °C. For intracellular cytokine and nuclear-factor staining, lung cells were stimulated with PMA and ionomycin for 6 h and brefeldin A for the last 4 h, as previously described (29). The cells were washed with nuclear-factor fixation and permeabilization buffer (BioLegend) and stained with anti-GM-CSF, anti-T-bet, anti-GATA3, anti-RORγt, and FoxP3 antibodies following the manufacturer's protocol. Flow cytometry data were acquired on a FACSCalibur (BD Biosciences) and analyzed with FlowJo software (Tree Star).

Quantitative real-time PCR. Total RNA was isolated from part of the right lung using an RNeasy Mini Kit (Qiagen, Hilden, Germany), followed by cDNA synthesis using a QuantiTect Reverse Transcription Kit (Qiagen). PCR reaction mixtures were prepared using the QuantiTect SYBR Green PCR Kit (Qiagen), followed by quantitative PCR on a PikoReal system (Thermo Fisher Scientific). The following primer pairs were used: gm-csf, 5'-CCAGCTCTGAATCCAGCTTCTC-3' (forward) and 5'-TCTCTCGTTTGTCTTCCGCTGT-3' (reverse); Il23p19, 5'-AATAATGTGCCCCGTATCCA-30 (forward) and 5'-GGATCCTTTGCAAGCAGAAC-3' (reverse). GAPDH was used as an internal control to normalize the amount of loaded complementary DNA (cDNA).

Generation of DCs from lung and bone-marrow cells in vitro. Total lung cells (1×10^6), total BM cells (1×10^6), and isolated lung $CD11b^{+}Ly6C^{high}$

cells (M-MDSCs) (1×10^5) from naïve SKG mice were cultured in RPMI 1640 medium supplemented with 10% FBS, 1% penicillin/streptomycin, 50 μM 2-ME, and 10 ng/ml GM-CSF, with or without 2.5 ng/ml rIL-4, as previously described (30). These cultures were maintained at 37 °C in 48-well plates in a 5% CO_2-humidified atmosphere. On day 3 of culture, the supernatant was gently removed and the medium was replaced with fresh medium containing GM-CSF with or without rIL-4. In some experiments. Anti-TGF-β antibody (αTGF) (5 μg/ml) was added when generating DCs from total lung cells. Cells were collected on day 5 and analyzed by flow cytometry.

Enzyme-linked immunosorbent assay. Total lung cells and BM cells were cultured as described above and the TGF-β1 levels in the culture supernatant were measured with commercial ELISA kits (R & D Systems) following the manufacturer's instructions.

Proliferation assay. Isolated spleen $CD4^+CD62L^+$ cells (naïve T cells) from SKG mice aged 3weeks were incubated with 10 μM CFSE-DA according to the manufacturer's protocol. CFSE-labeled naïve T cells (1×10^5) in 200 μl of medium were cultured for 3 days in a 96-well flat-bottomed plate pre-coated with 10 μg/ml anti-CD3 antibody and 5 μg/ml anti-CD28 antibody with or without lung MDSCs, $CD11b^+Gr1^{dim}$ cells, or BM MDSCs obtained from ZyA-treated SKG mice, or with in-vitro-generated $CD11b^+Gr1^{dim}$ cells or BMDCs. The naïve T-cell proliferation was determined by measuring the CFSE fluorescence using flow cytometry.

Adoptive Transfer experiments. Total lung cells from ZyA-treated SKG mice were cultured with GM-CSF and IL-4 for 7 days as described above

in order to generate $CD11b^{+}Gr1^{dim}$ cells. The cells were stimulated with ZyA (5 μg/ml) for the last 2 days. The in vitro-generated $CD11b^{+}Gr1^{dim}$ cells (5×10^{5} cells/mouse) were isolated by using FACSAria III and transferred into ZyA-treated SKG mice through the tail vein once every two weeks for 3 months. SAL was injected as a control.

Statistical analysis. Results are expressed as the mean ± SEM. All analyses were performed using GraphPad Prism 5 software (GraphPad). Statistical comparisons between two groups were performed using Student's t-test in the case of normal distribution or the Mann-Whitney U-test in the case of non-normal distribution. For multiple comparisons, the Kruskal-Wallis test was used. Pearson's or Spearman's correlation coefficient was calculated for the correlations performed. P values <0.05 were considered statistically significant.

RESULTS

ZyA-treated SKG mice developed chronic, progressive, and severe ILD. ZyA-treated SKG mice can develop ILD, which is characterized by inflammatory-cell infiltration. Although the inflammatory-cell infiltration into interstitial spaces was mild at 8 weeks after ZyA-injection, a massive infiltration resembling organizing pneumonia was observed extending into the interstitial and alveolar spaces at 12 weeks after ZyA-injection (Figure 1 A and D). The mice started to develop arthritis 6 weeks after the ZyA-injection, which worsened thereafter (Figure 1 B), and began losing body weight 8 weeks after the ZyA-injection (Figure 1C). The severity of ILD was correlated with the loss of

body weight, but not with the arthritis score (Supplemental Figure 1).

Since not all of the ZyA-treated SKG mice developed severe ILD, we examined the mice 12 weeks after ZyA-injection and scored the severity of ILD according to the diffusely affected area visible with H&E staining: HS0 (normal), HS1 (10-30%), HS2 (30-60%), or HS3 (>60%) (Figure 1D). This analysis revealed that about half of the ZyA-treated SKG mice developed HS2-level ILD, and about 25% developed HS3-level ILD. High-power views of H&E staining showed the infiltration of mononuclear and polynuclear cells into the interstitial space, and revealed the presence of unique cells with a large, bright cytoplasm only in specimens from ZyA-treated mice with HS3 (ZyA-HS3) (Figure 1 E, arrow). Masson's trichrome staining showed that the ZyA-treated SKG mice developed mild fibrosis but no honeycombing (Figure 1F).

MDSCs were increased in ZyA-treated SKG lungs, while CD11b^{+}Gr1^{dim} cells were expanded only in ZyA-HS3 lungs. We next investigated the characteristics of the lung-infiltrating cells in the ZyA-treated mice. The total number of infiltrating cells were increased significantly in the ZyA-HS3 lungs (Figure 2A). Flow cytometry revealed a higher proportion of CD11b^{+}Gr1^{+} cells (MDSCs) in the lungs of ZyA-treated mice than in those of SAL-treated mice. Interestingly, the proportion of CD11b^{+}Gr1^{dim} cells was elevated only in ZyA-HS3 lungs (Figure 2B and C). We further analyzed these subpopulations by gating for CD11b-positive cells. Although there was no significant difference in the proportion of CD11b^{+}Ly6C^{high}Ly6G^{-} cells (M-MDSCs) or CD11b^{+}Ly6C^{low}Ly6G^{+} cells (PMN-MDSCs) between ZyA-HS1 and ZyA-HS3 specimens, the proportion of CD11b^{+}Ly6C^{-}Ly6G^{int} cells were

increased only in the ZyA-HS3 lungs (Figure 2D). These results suggested that $CD11b^{+}Gr1^{dim}$ cells and $CD11b^{+}Ly6C^{-}Ly6G^{int}$ cells might be the same population.

We next analyzed the CD11c expression in MDSCs and $CD11b^{+}Gr1^{dim}$ cells, and found that MDSCs and $CD11b^{+}Gr1^{dim}$ cells from ZyA-HS3 lungs expressed significantly more CD11c than did those in control specimens (Figure 2E–H). CD11c was expressed more strongly in $CD11b^{+}Gr1^{dim}$ cells than in MDSCs (Figure 2E–H), and the $CD11b^{+}Gr1^{dim}$ cells did not express F4/80 (Figure 2G). May-Giemsa staining revealed that $CD11b^{+}Gr1^{dim}$ cells were morphologically immature dendritic cell-like (Figure 2I). $CD11b^{+}Gr1^{dim}$ cells were not detected in the spleen or BM of ZyA-treated SKG mice with HS3 lungs (Figure 2J). As few of MDSCs express CD11c, these results indicated that $CD11b^{+}Gr1^{dim}$ cells and MDSCs might be different populations, and that $CD11b^{+}Gr1^{dim}$ cells would be a cell population differentiating into DCs in the severely inflamed lung.

GM-CSF-producing Th17 cells, ILC1s, and ILC3s were increased in ZyA-treated SKG lungs. As GM-CSF is known to be important in DC differentiation, we next investigated GM-CSF expression in the lungs of ZyA-treated SKG mice. Quantitative RT-PCR revealed that GM-CSF was significantly elevated in the lungs of ZyA-treated SKG mice compared to control (Figure 3A). The levels of IL-23p19, which induces the differentiation of Th17 cells and group 3 ILCs (ILC3s), were also elevated in the ZyA-treated mice (Figure 3A). $CD4^{+}$ T cells and ILCs were recently identified as sources of GM-CSF (31-35); thus, we first analyzed $CD4^{+}$ T cells as a GM-CSF source and

found that the numbers of total $CD4^+$ cells and $ROR\gamma t^+CD4^+$ cells were significantly elevated in ZyA-HS3 lungs (Figure 3B). We also found significantly elevated numbers of $GM\text{-}CSF^+CD4^+$ cells and $GM\text{-}CSF^+ROR\gamma t^+CD4^+$ cells in ZyA-HS2 and ZyA-HS3 lungs (Figure 3C and D). We next examined ILCs, defined as $Lin^-CD90.2^+$ cells, in the total lymphoid-cell population, as previously described (36) (Figure 3E). ILC1s, ILC2s, and ILC3s were classified by T-bet, GATA3, and RORγt expression, respectively. The total numbers of ILCs, $T\text{-}bet^+$ ILCs (ILC1s), and $ROR\gamma t^+$ ILCs (ILC3s) were significantly increased in the ZyA-HS3 lung (Figure 3F). In addition, $GM\text{-}CSF^+$ ILCs, $GM\text{-}CSF^+$ ILC1s, and $GM\text{-}CSF^+$ ILC3s were significantly elevated in the ZyA-HS2 and ZyA-HS3 lungs (Figure 3G and H). Thus, the numbers of GM-CSF-producing Th17 cells, ILC1s, and ILC3s were significantly increased in the lungs of ZyA-treated SKG mice.

$CD11b^+Gr1^{dim}$ cells were differentiated from M-MDSCs in vitro by GM-CSF and IL-4 stimulation. The generation of DCs from BM cells in vitro using GM-CSF is well established (30,37). To determine whether DCs could be generated from lung cells using GM-CSF, we cultured total lung cells with GM-CSF in vitro in the presence or absence of IL-4. GM-CSF alone induced $CD11b^+Gr1^{dim}$ cells from total lung cells, and adding IL-4 facilitated the differentiation (Figure 4A and B). The in-vitro-generated $CD11b^+Gr1^{dim}$ cells expressed high levels of CD11c (Figure 4A). Microscopic examination and flow cytometry based on forward scatter (FSC) and side scatter (SSC) parameters revealed that the in-vitro-generated $CD11b^+Gr1^{dim}$ cells and the $CD11b^+Gr1^{dim}$ cells ex vivo were larger than lymphocytes (Figure 4C and D). Histology showed the presence of cells with a large, bright cytoplasm which would be

$CD11b^{+}Gr1^{dim}$ cells in vivo in the ZyA-HS3 lung (Figure 4D). These results indicated that the in-vitro-generated $CD11b^{+}Gr1^{dim}$ cells and the $CD11b^{+}Gr1^{dim}$ cells found in the ZyA-HS3 lung were similar populations.

We next investigated which cell populations differentiated into $CD11b^{+}Gr1^{dim}$ cells. Although some MDSCs expressed CD11c in severe ILD (ZyA-HS3), the differentiation of $CD11b^{+}Gr1^{dim}$ cells was not observed when total MDSCs were stimulated with GM-CSF and IL-4 (Supplemental Figure 2A). One study showed that splenic $CD11b^{+}Ly6G^{-}Ly6C^{high}$ cells (M-MDSCs) can differentiate into $CD11b^{+}CD11c^{+}F4/80^{+}$ cells (DCs and macrophages) when stimulated by GM-CSF (38). $CD11b^{+}Gr1^{dim}$ cells were induced when $CD11b^{+}Ly6C^{high}$ cells (M-MDSC) isolated from the lung were cultured with GM-CSF and IL-4 (Figure 4E and F). $CD11b^{+}Ly6C^{low}$ cells (PMN-MDSCs) did not differentiate to $CD11b^{+}Gr1^{dim}$ cells (Supplemental Figure 2B). These results indicated that $CD11b^{+}Gr1^{dim}$ cells were differentiated from M-MDSCs.

$CD11b^{+}Gr1^{dim}$ cells were tolDC-like cells with immunosuppressive characteristics. To elucidate the role of the $CD11b^{+}Gr1^{dim}$ cells in ILD, we examined the effect of $CD11b^{+}Gr1^{dim}$ cells isolated from the ZyA-HS3 lung on T-cell proliferation. A T-cell proliferation assay revealed that the $CD11b^{+}Gr1^{dim}$ cells, like MDSCs from the lung or bone marrow, suppressed naïve T-cell proliferation (Figure 5A). To clarify the difference between $CD11b^{+}Gr1^{dim}$ cells and MDSCs from the lungs, we evaluated their PD-L1 and CD80 expression. The $CD11b^{+}Gr1^{dim}$ cells and MDSCs in ZyA-HS3 expressed significantly more PD-L1 than did those in SAL-treated SKG mice, and the $CD11b^{+}Gr1^{dim}$ cells expressed more PD-L1 than did MDSCs (Figure 5B). The CD80 levels were

significantly higher in $CD11b^{+}Gr1^{dim}$ cells from ZyA-HS3 than those from SAL-treated mice, while the CD80 expression was comparable in MDSCs from ZyA-HS3 and SAL-treated mice (Figure 5B,D). $CD11b^{+}Gr1^{dim}$ cells from ZyA-HS3 expressed higher PD-L1 and CD80 compared to those from ZyA-HS1 and HS2 (Figure 5C,E). We termed these tolDC-like $CD11b^{+}Gr1^{dim}$ cells "$CD11b^{+}Gr1^{dim}$tolDC-like cells (LCs)" because of their phenotype and function.

We next generated $CD11b^{+}Gr1^{dim}$tolDC-LCs and BMDCs in vitro and investigated their effect on T-cell proliferation. The in-vitro-generated $CD11b^{+}Gr1^{dim}$tolDC-LCs also suppressed naïve T-cell proliferation; in contrast, the in-vitro-generated BMDCs facilitated T-cell proliferation (Figure 5F). The PD-L1 levels were higher in the in-vitro-generated $CD11b^{+}Gr1^{dim}$tolDC-LCs than in the in-vitro-generated BMDCs, while the CD80 levels did not differ between these cells (Figure 5G). These results indicated that the in-vitro-generated $CD11b^{+}Gr1^{dim}$tolDC-LCs were tolerogenic, and the in-vitro-generated BMDCs were immunogenic.

In order to elucidate why lung cell-culture induces tolerogenic DC while BM cell-culture generates immunogenic DC, we studied TGF-β levels in the culture supernatant. TGF-β concentrations were higher in the supernatant of lung cell-culture than that of BM cell-culture (Figure 5H). We then cultured total lung cells with GM-CSF and IL-4 in the presence or absence of anti-TGF-β antibody (αTGF) for 5 days, to generate $CD11b^{+}Gr1^{dim}$tolDC-LCs (defined as αTGF-$CD11b^{+}Gr1^{dim}$tolDC-LCs). Then, naïve T cells were co-cultured with αTGF-$CD11b^{+}Gr1^{dim}$tolDC-LCs. The αTGF-$CD11b^{+}Gr1^{dim}$tolDC-LCs partially lost their suppressive function on T cell proliferation (Figure 5I). These results

indicate that TGF-β is one of the key factors for CD11b^{+}Gr1^{dim} cells to be tolerogenic.

CD11b^{+}Gr1^{dim}tolDC-LCs suppressed the progression of ILD in ZyA-treated SKG mice. To further define the suppressive role of CD11b^{+}Gr1^{dim}tolDC-LCs in vivo, we performed an adoptive transfer experiment. Total lung cells were cultured with GM-CSF and IL-4 in vitro, and CD11b^{+}Gr1^{dim}tolDC-LCs were purified by flow cytometry (Figure 6A). We adoptively transferred the in-vitro-generated CD11b^{+}Gr1^{dim}tolDC-LCs into the ZyA-treated SKG mice every two weeks for three months (Figure 6B). We revealed that adoptive transfer of the in vitro-generated CD11b^{+}Gr1^{dim}tolDC-LCs significantly decreased the severity of ILD in ZyA-treated SKG mice (Figure 6C, D). Taken together, these results suggest that CD11b^{+}Gr1^{dim}tolDC-LCs are induced in the severely inflamed lung to control excessive inflammation.

DISCUSSION

In this study, we identified unique CD11b^{+}Gr1^{dim}tolDC-like cells and showed that the proportion of MDSCs was elevated in the lungs of SKG mice with ZyA-induced ILD. TolDCs generally express CD11c, high levels of PD-L1, and low levels of CD80. As the CD11b^{+}Gr1^{dim} cells we detected expressed relatively low levels of CD11c and high levels of PD-L1 and CD80, we termed these cells CD11b^{+}Gr1^{dim}tolDC-“like” cells. CD11b^{+}Gr1^{dim}tolDC-LCs, which were induced by GM-CSF from M-MDSCs, suppressed naïve T-cell proliferation in vitro. Th17 cells, ILC1s, and ILC3s produced GM-CSF in vivo. Furthermore,

adoptive transfer of $CD11b^{+}Gr1^{dim}$tolDC-LCs significantly suppressed the progression of ILD in SKG mice.

About half of the $CD11b^{+}Gr1^{dim}$tolDC-LCs expressed CD11c, while few of the MDSCs expressed CD11c. These results indicate that the $CD11b^{+}Gr1^{dim}$ tolDC-LCs would be a cell population which are differentiating into DCs. The $CD11b^{+}Gr1^{dim}$tolDC-LCs expressed PD-L1 and suppressed the proliferation of naïve T cells, suggesting that $CD11b^{+}Gr1^{dim}$tolDC-LCs can be classified as a subset of tolDCs. TolDCs generally exert immunosuppressive activity by expressing inhibitory molecules such as PD-L1, PD-L2, and Fas-ligand, by secreting anti-inflammatory cytokines such as IL-10 and TGF-β, and by upregulating IDO (indole amine 2,3-deoxygenate) (9,22). $CD11b^{+}Gr1^{dim}$tolDC-LCs are different from so-called tolDCs in that they expressed high levels both of PD-L1 and CD80 while tolDCs generally express high levels of PD-L1 and low levels of CD80.

$CD11b^{+}Gr1^{dim}$tolDC-LCs are distinct from MDSCs. MDSCs are phenotypically defined as $CD11b^{+}Gr1^{+}$ cells. As the $CD11b^{+}Gr1^{dim}$tolDC-LCs expressed both CD11b and Gr1, we examined their characteristics to determine whether they were a type of MDSC. Microscopic examination and flow cytometric analysis based on FSC and SSC parameters revealed that the $CD11b^{+}Gr1^{dim}$tolDC-LCs were larger than MDSCs. Although MDSCs were distributed into $CD11b^{+}Ly6C^{high}Ly6G^{-}$ (M-MDSC) or $CD11b^{+}Ly6C^{low}Ly6G^{+}$ (PMN-MDSC) populations, the $CD11b^{+}Gr1^{dim}$tolDC-LCs were distributed into the $CD11b^{+}Ly6G^{int}Ly6C^{-}$ population. Furthermore, $CD11b^{+}Gr1^{dim}$tolDC-LCs expressed higher levels of PD-L1 and CD80 than did MDSCs. These results

indicate that the CD11b^{+}Gr1^{dim}tolDC-LCs are not a type of MDSCs.

Various factors are known to induce tolDCs from BMDCs in vitro, including the cytokines; IL-10, IFN-γ, and TGF-β, the drugs; dexamethasone, tacrolimus, and mycophenolate, and the organic molecules; vitamin D3, intravenous immunoglobulin, and salicylate (12). In our study, CD11b^{+}Gr1^{dim}tolDC-LCs were induced from total lung cells by GM-CSF (and IL-4) without the stimulation of these additional factors. A previous report demonstrated that pulmonary stromal cells induced the generation of tolDCs (39); in that study, TGF-β from the stromal cells was found to be involved in the differentiation of BM-derived tolDCs in vitro. We showed that TGF-β concentration was higher in the supernatant of lung cell-culture than that of BM cell-culture, and that αTGF-CD11b^{+}Gr1^{dim}tolDC-LCs partially lost their suppressive function on T cell proliferation in vitro. These results support that TGF-β produced by lung interstitial cells is one of the key factors for CD11b^{+}Gr1^{dim}tolDC-LCs to be tolerogenic. The induction of CD11b^{+}Gr1^{dim}tolDC-LCs by GM-CSF and IL-4 from isolated M-MDSCs in vitro was weak compared to their induction from total lung cells, which might imply that lung interstitial cell-derived TGF-β contributes to the induction of CD11b^{+}Gr1^{dim}tolDC-LCs.

The molecular mechanism of suppressive effects of CD11b^{+}Gr1^{dim}tolDC-LCs are still to be elucidated. Although the in-vitro-generated CD11b^{+}Gr1^{dim}tolDC-LCs expressed higher levels of PD-L1 compared to the in vitro-generated BMDC, the blockade of PD-L1 in CD11b^{+}Gr1^{dim}tolDC-LCs did not restore the ability to proliferate T cells (data was not shown).

Some investigators have reported that CD11b^{+}Gr1^{int}F4/80^{+} cells regulate inflammation in the lung by secreting IL-10 (40,41). These CD11b^{+}Gr1^{int}F4/80^{+}

cells express Ly6C^{low}Ly6G^{int} and are recognized as a PMN-MDSC subset. These cells are distinct from the CD11b^{+}Gr1^{dim}tolDC-LCs in our study, which are not MDSCs and express low levels of F4/80 but high levels of CD11c. Recently, another group described SSC^{low}CD11b^{+}Gr1^{dim} cells with immunosuppressive function via a nitric oxide-dependent mechanism in the liver of obese mice (42). These SSC^{low}CD11b^{+}Gr1^{dim} cells are Ly6C^{high}Ly6G^{-}, express CD80 and PD-L1 but not CD11c, and are recognized as an M-MDSC subset. The SSC^{low}CD11b^{+}Gr1^{dim} cells are morphologically small and distinct from granulocytes. The Gr1^{dim}tolDC-LCs in our study are distinguished from the SSC^{low}CD11b^{+}Gr1^{dim} cells by their large size and expression of Ly6C^{-}Ly6G^{int} and CD11c. Thus, although the CD11b^{+}Gr1^{dim}tolDC-LCs described in this study share some similarities in name with CD11b^{+}Gr1^{int}F4/80^{+} and SSC^{low}CD11b^{+}Gr1^{dim} cells, the CD11b^{+}Gr1^{dim}tolDC-LCs are a distinct cell population.

A recent report demonstrated that GM-CSF produced by Th cells is critical for the development of ILD in SKG mice, and that the progress of ILD is inhibited by neutralizing GM-CSF with anti-GM-CSF antibodies (34). In that study, CD11b^{+}Gr1^{+} cells and CD11b^{+}Gr1^{-} cells are immunogenic and are increased in the lungs of ZyA-treated SKG mice, and characterized these cells as neutrophils and macrophages/monocytes, respectively. However, in our study, we identified CD11b^{+}Gr1^{+} cells as MDSCs and CD11b^{+}Gr1^{dim} cells as tolDC-like cells that proliferated in the severely inflamed ILD lung. Indeed, GM-CSF is immunogenic, as described by as Shiomi et al., but our results demonstrated that GM-CSF also induced immunosuppressive cells such as

MDSCs and tolDC-like cells. Considering the origin and role of $CD11b^{+}Gr1^{dim}$tolDC-LCs, it is possible that they function as a suppressive last resort if MDSCs cannot suppress the inflammation.

Some $CD4^{+}$ T cells produce GM-CSF under inflammatory conditions (31, 32). In our study, ZyA-HS2 and ZyA-HS3 lungs had a high proportion of GM-CSF-producing $CD4^{+}$ T cells and $ROR\gamma t^{+}CD4^{+}$ T cells (Th17 cells), consistent with previous reports. Recent reports have demonstrated that ILC3s produce GM-CSF in acute intestinal inflammation (35,43,44). Thus, we investigated the GM-CSF production by ILCs in the SKG lung, revealed that GM-CSF–producing ILC1s and ILC3s were increased in the lung of ZyA-treated SKG mice. Although both $CD4^{+}$ T cells and ILCs produced GM-CSF, they appeared to act in different stages of ILD: the proportion of ILC1s and ILC3s increased mostly at HS1, while the proportion of Th17 cells increased at HS3, although the actual counts of Th17 cells and ILCs were most strongly elevated at HS3 (Supplemental Figure 3A and B). These findings might indicate that ILCs and Th17 cells act in the early and late stages of ILD, respectively, and that Th17 cells, ILC1s, and ILC3s contribute to the development of ILD and the induction of $CD11b^{+}Gr1^{dim}$tolDC-LCs by producing GM-CSF. To our knowledge, this is the first report showing the presence of GM-CSF-producing ILCs in the lungs.

In summary, we identified a new cell population, $CD11b^{+}Gr1^{dim}$tolDC-LCs, in the severely inflamed lungs of ZyA-treated SKG mice. Th17 cells, ILC1s and ILC3s produced GM-CSF, which in turn could induce $CD11b^{+}Gr1^{dim}$tolDC-LCs from M-MDSC to reduce inflammation. We also demonstrated that adoptive transfer of $CD11b^{+}Gr1^{dim}$tolDC-LCs suppressed the development of ILD in ZyA-

treated SKG mice. Although further studies are needed to elucidate the mechanism how $CD11b^{+}Gr1^{dim}$tolDC-LCs suppress other immune cells involved in lung inflammation/fibrosis, the unique cells could play a potent suppressive role in the lung lesion of SKG mice.

ACKNOWLEDGMENTS

The authors thank Shino Tanaka (Department Rheumatology and Clinical Immunology, Kobe University Graduate School of Medicine) for providing technical assistance.

AURTHOR CONTRIBUTIONS

Akio Morinobu had full access to all of the data in the study and takes responsibility for the integrity of the data and the accuracy of the data analysis.

Study conception and design: Sho Sendo, Jun Saegusa, and Akio Morinobu.

Acquisition of data: Sho Sendo, and Takaichi Okano.

Analysis and interpretation of data: Sho Sendo, Soshi Takahashi, Kengo Akashi, Jun Saegusa, and Akio Morinobu.

REFERENCES

1. Turesson C, Matteson EL, Colby TV, Vuk-Pavlovic Z, Vassallo R, Weyand CM, et al. Increased CD4+ T cell infiltrates in rheumatoid arthritis-associated interstitial pneumonitis compared with idiopathic interstitial pneumonitis. Arthritis Rheum 2005; 52:73–79.

2. Shimizu Y, Kuwabara H, Ono A, Higuchi S, Hisada T, Dobashi K, et al. Intracellular Th1/Th2 balance of pulmonary CD4(+) T cells in patients with active interstitial pneumonia evaluated by serum KL-6. Immunopharmacol Immunotoxicol 2006;28:295-304.
3. Yoshinouchi T., Ohtsuki Y, Ueda R, Sato S, Ueda N. Myofibroblasts and S-100 protein positive cells in idiopathic pulmonary fibrosis and rheumatoid arthritis-associated interstitial pneumonia. Eur. Respir. J 199;14:579–84.
4. Kim EJ, Collard HR, King Jr. TE. Rheumatoid arthritis-associated interstitial lung disease: the relevance of histopathologic and radiographic pattern. Chest 2009;136:1397-405.
5. de Lauretis A, Veeraraghavan S, Renzoni E. Review series: Aspects of interstitial lung disease: connective tissue disease-associated interstitial lung disease: how does it differ from IPF? How should the clinical approach differ? Chron. Respir 2011;8:53–82.
6. Ota M, Iwasaki Y, Harada H, Sasaki O, Nagafuchi Y, Nakachi S, et al. Efficacy of intensive immunosuppression in exacerbated rheumatoid arthritis-associated interstitial lung disease. Mod Rheumatol 2016. doi:10.3109/14397595.2016.1173816.
7. Sakaguchi N, Takahashi T, Hata H, Nomura T, Tagami T, Yamazaki S, et al. Altered thymic T-cell selection due to a mutation of the ZAP-70 gene causes autoimmune arthritis in mice. Nature 2003;426:454–60.
8. Sakaguchi S, Sakaguchi N, Yoshitomi H, Hata H, Takahashi T, Nomura T. Spontaneous development of autoimmune arthritis due to genetic anomaly of T cell signal transduction: Part 1. Semin. Immunol 2006;18:199–206.

9. Merad M, Sathe P, Helft J, Miller J, Mortha A. The dendritic cell lineage: ontogeny and function of dendritic cells and their subsets in the steady state and the inflamed setting. Annu. Rev. Immunol 2013;31:563–604.
10. Steinman, RM. The dendritic cell system and its role in immunogenicity. Annu Rev Immunol 1991;9:271-96.
11. Jonuleit H, Schmitt E, Schuler G, Knop J, Enk AH. Induction of interleukin 10-producing, nonproliferating CD4(+) T cells with regulatory properties by repetitive stimulation with allogeneic immature human dendritic cells. J Exp Med 2000;192:1213-22.
12. Takenaka MC, Quintana FJ. Tolerogenic dendritic cells. Semin. Immunopathol 2016. doi:10.1007/s00281-016-0587-8.
13. Devi KS, Anandasabapathy N. The origin of DCs and capacity for immunologic tolerance in central and peripheral tissues. Semin Immunopathol 2016. DOI:10.1007/s00281-016-0602-0.
14. Sharma MD, Baban B, Chandler P, Hou DY, Singh N, Yagita H, et al. Plasmacytoid dendritic cells from mouse tumor-draining lymph nodes directly activate mature Tregs via indoleamine 2,3-dioxygenase. J Clin Invest 2007;117:2570-82.
15. Goubier A, Dubois B, Gheit H, Joubert G, Villard-Truc F, Asselin-Paturel C, et al. Plasmacytoid dendritic cells mediate oral tolerance. Immunity 2008;29:464-75.
16. Gomez de Agüero M, Vocanson M, Hacini-Rachinel F, Taillardet M, Sparwasser T, Kissenpfennig A, et al. Langerhans cells protect from allergic contact dermatitis in mice by tolerizing CD8(+) T cells and activating

Foxp3(+) regulatory T cells. J Clin Invest 2012;122:1700-11.

17. Khare A, Krishnamoorthy N, Oriss TB, Fei M, Ray P, Ray A. Cutting edge: inhaled antigen upregulates retinaldehyde dehydrogenase in lung CD103+ but not plasmacytoid dendritic cells to induce Foxp3 de novo in CD4+ T cells and promote airway tolerance. J Immunol 2013;191:25-9.
18. Gordon JR, Ma Y, Churchman L, Gordon SA, Dawicki W. Regulatory dendritic cells for immunotherapy in immunologic diseases. Front. Immunol 2014;5:7. doi: 10.3389/fimmu.2014.00007.
19. Tsoumakidou M, Tousa S, Semitekolou M, Panagiotou P, Panagiotou A, Morianos I, et al. Tolerogenic signaling by pulmonary $CD1c^{+}$ dendritic cells induces regulatory T cells in patients with chronic obstructive pulmonary disease by IL-27/IL-10/inducible costimulator ligand. J. Allergy Clin. Immunol 2014;134:944–954.e8.
20. Liu JY, Li LY, Yang XZ, Li J, Zhong G, Wang J, et al. Adoptive transfer of dendritic cells isolated from helminth-infected mice enhanced T regulatory cell responses in airway allergic inflammation. Parasite Immunol 2011;33:525–34.
21. Torres-Aguilar H, Blank M, Jara LJ, Shoenfeld Y. Tolerogenic dendritic cells in autoimmune diseases: crucial players in induction and prevention of autoimmunity. Autoimmun Rev 2010;10:8-17.
22. Yoo S, Ha SJ. Generation of Tolerogenic Dendritic Cells and Their Therapeutic Applications. Immune 2016;16:52–60.
23. Bronte V, Brandau S, Chen SH, Colombo MP, Frey AB, Greten TF, et al. Recommendations for myeloid-derived suppressor cell nomenclature and

characterization standards. Nat. Commun 2016;7:12150.

24. Ioannou M, Alissafi T, Lazaridis I, Deraos G, Matsoukas J, Gravanis A, et al. Crucial role of granulocytic myeloid-derived suppressor cells in the regulation of central nervous system autoimmune disease. J Immunol 2012. 188:1136-46.
25. Nishimura K, Saegusa J, Matsuki F, Akashi K, Kageyama G, Morinobu A. Tofacitinib facilitates the expansion of myeloid-derived suppressor cells and ameliorates arthritis in SKG mice. Arthritis Rheumatol 2015;67:893–902.
26. Bell GM, Anderson AE, Diboll J, Reece R, Eltherington O, Harry RA, et al. Autologous tolerogenic dendritic cells for rheumatoid and inflammatory arthritis. Ann Rheum Dis 2016. 76(1):227-234.
27. Yoshitomi H, Sakaguchi N, Kobayashi K, Brown GD, Tagami T, Sakihama T, et al. A role for fungal {beta}-glucans and their receptor Dectin-1 in the induction of autoimmune arthritis in genetically susceptible mice. J. Exp. Med 2005. 201:949–60.
28. Wakasa-Morimoto C, Toyosaki-Maeda T, Matsutani T, Yoshida R, Nakamura-Kikuoka S, Maeda-Tanimura M, et al. Arthritis and pneumonitis produced by the same T cell clones from mice with spontaneous autoimmune arthritis. Int. Immunol 2008;20:1331–42.
29. Nishikomori R, Ehrhardt RO, Strober W. T helper type 2 cell differentiation occurs in the presence of interleukin 12 receptor beta2 chain expression and signaling. J. Exp. Med 2000;191:847–58.
30. Inaba K, Inaba M, Romani N, Aya H, Deguchi M, Ikehara S, et al. Generation of large numbers of dendritic cells from mouse bone marrow

cultures supplemented with granulocyte/macrophage colony-stimulating factor. J. Exp. Med 1992;176:1693–702.

31. Codarri L, Gyülvészi G, Tosevski V, Hesske L, Fontana A, Magnenat L, et al. RORγt drives production of the cytokine GM-CSF in helper T cells, which is essential for the effector phase of autoimmune neuroinflammation. Nat. Immunol 2011;12:560–67.
32. El-Behi M, Ciric B, Dai H, Yan Y, Cullimore M, Safavi F, et al. The encephalitogenicity of T(H)17 cells is dependent on IL-1- and IL-23-induced production of the cytokine GM-CSF. Nat. Immunol 2011;12:568–75.
33. Lukens JR, Barr MJ, Chaplin DD, Chi H, Kanneganti TD. Inflammasome-derived IL-1β regulates the production of GM-CSF by CD4(+) T cells and γδ T cells. J Immunol 2012;188:3107–15.
34. Shiomi A, Usui T, Ishikawa Y, Shimizu M, Murakami K, Mimori T. GM-CSF but not IL-17 is critical for the development of severe interstitial lung disease in SKG mice. J. Immunol 2014;193:849–59.
35. Pearson C, Thornton EE, McKenzie B, Schaupp AL, Huskens N, Griseri T, et al. ILC3 GM-CSF production and mobilisation orchestrate acute intestinal inflammation. Elife 2016. doi:10.7554/eLife.10066.
36. Spencer SP, Wilhelm C, Yang Q, Hall JA, Bouladoux N, Boyd A, et al. Adaptation of innate lymphoid cells to a micronutrient deficiency promotes type 2 barrier immunity. Science 2014;343:432–7.
37. Dong Y, Arif AA, Poon GF, Hardman B, Dosanjh M, Johnson P. Generation and Identification of GM-CSF Derived Alveolar-like Macrophages and Dendritic Cells From Mouse Bone Marrow. J. Vis. Exp 2016.

doi:10.3791/54194.

38. Youn JI, Nagaraj S, Collazo M, Gabrilovich DI. Subsets of myeloid-derived suppressor cells in tumor-bearing mice. J. Immunol 2008;181:5791–802.
39. Li Q, Guo Z, Xu X, Xia S, Cao X. Pulmonary stromal cells induce the generation of regulatory DC attenuating T-cell-mediated lung inflammation. Eur. J. Immunol 2008;38:2751–61.
40. Arora M, Poe SL, Oriss TB, Krishnamoorthy N, Yarlagadda M, Wenzel SE, et al. TLR4/MyD88-induced CD11b+Gr-1 int F4/80+ non-migratory myeloid cells suppress Th2 effector function in the lung. Mucosal Immunol 2010;3:578–93.
41. Poe SL, Arora M, Oriss TB, Yarlagadda M, Isse K, Khare A, et al. STAT1-regulated lung MDSC-like cells produce IL-10 and efferocytose apoptotic neutrophils with relevance in resolution of bacterial pneumonia. Mucosal Immunol 2013;6:189–99.
42. Yao L, Abe M, Kawasaki K, Akbar SM, Matsuura B, Onji M, et al. Characterization of Liver Monocytic Myeloid-Derived Suppressor Cells and Their Role in a Murine Model of Non-Alcoholic Fatty Liver Disease. PLoS One 2016;11:e0149948. doi:10.1371/journal.pone.0149948.
43. Mortha A, Chudnovskiy A, Hashimoto D, Bogunovic M, Spencer SP, Belkaid Y, et al. Microbiota-dependent crosstalk between macrophages and ILC3 promotes intestinal homeostasis. Science 2014;517:293–301.
44. Artis D, Spits H. The biology of innate lymphoid cells. Nature 2015;517:293-301.

FIGURE LEGENDS

Figure 1. Zymosan A–treated SKG mice developed chronic, progressive, and severe ILD. **A,** Progression of ILD over time, assessed by the percentage of the affected area in SKG mice injected with zymosan A (ZyA) or normal saline (SAL) (day 0: SAL n=6, ZyA n=6; day 28: SAL n=5, ZyA n=4; day 56: SAL n=5, ZyA n=5; day 84: SAL n=4, ZyA n=5). **B,** Changes in the arthritis score over time in SKG mice treated with ZyA (n=28) or SAL (n=9). **C,** Changes in body weight after i.p. injection of ZyA (n=28) or SAL (n=9). **D,** Hematoxylin and eosin staining of lungs from SKG mice 12 weeks after ZyA or SAL injection, showing representative images of histological scores (HS) in ZyA-treated SKG mice. **E,** Nonspecific-pneumonia-like inflammatory-cell infiltrations were observed in HS1 and HS2, and massive infiltrations of inflammatory cells in HS3. Unique cells with a large, bright nucleus were observed only in HS3 (arrow). **F,** Masson's trichrome staining showed mild fibrosis in the lung from ZyA-treated SKG mice. Data shown in B and C are representative of at least two independent experiments. Data are shown as mean ± SEM. *, $P < 0.05$, Student's t tests.

Figure 2. $CD11b^{+}Gr1^{+}$ cells (MDSCs) were increased in the ZyA-HS1 and HS2 lungs, while $CD11b^{+}Gr1^{dim}$ cells were expanded only in the ZyA-HS3 lungs. The lung-Infiltrating cells 12 weeks after ZyA or SAL injection. **A,** The total cell counts of each histological score (HS) (SAL n=9, ZyA-HS1 n=8, ZyA-HS2 n=15, ZyA-HS3 n=7). **B,** Representative flow cytometry plots show the distribution of $CD11b^{+}Gr1^{+}$ cells and $CD11b^{+}Gr1^{dim}$ cells for each HS classification. **C,** The proportion of $CD11b^{+}Gr1^{+}$ cells and $CD11b^{+}Gr1^{dim}$ cells in each HS. (SAL n=8,

ZyA-HS1 n=7, ZyA-HS2 n=14, ZyA-HS3 n=6). **D,** Lung cells were gated on CD11b expression and stained for Ly6C and Ly6G. $Ly6C^{-}Ly6G^{int}$ cells existed only in the ZyA-HS3 lung. **E, F,** Approximately 20% of the $CD11b^{+}Gr1^{+}$ cells from ZyA-HS3 lungs expressed CD11c (SAL n=8, ZyA-HS3 n=10). **G, H,** About half of the $CD11b^{+}Gr1^{dim}$ cells from ZyA-HS3 lungs expressed CD11c (SAL n=9, ZyA-HS3 n=10). **I,** May-Giemsa staining of $CD11b^{+}Gr1^{dim}$ cells. **J,** $CD11b^{+}Gr1^{dim}$ cells were not observed in the BM or spleen. Data are shown as mean ± SEM. *, $P < 0.05$; **, $P < 0.01$; ***, $P < 0.001$, Kruskal-Wallis tests (**A, C**). Mann-Whitney U-tests (**F, H**).

Figure 3. GM-CSF-producing Th17 cells, ILC1s, and ILC3s were increased in the lungs of ZyA-treated SKG mice. **A,** Quantitative RT-PCR analysis revealed that the relative mRNA expression of GM-CSF and IL-23p19 was elevated in the ZyA lung (SAL n=5, ZyA n=5). **B,** The total counts of $CD4^{+}$ cells and $ROR\gamma t^{+}CD4^{+}$ cells were elevated in the ZyA-HS3 lungs. **C,** Lung cells were stained with anti-CD4 and anti-GM-CSF antibodies. Representative results are shown. **D,** The numbers of $GM\text{-}CSF^{+}CD4^{+}$ cells and $GM\text{-}CSF^{+}ROR\gamma t^{+}CD4^{+}$ cells were elevated in ZyA-HS2,3 lungs (SAL n=5, ZyA-HS2,3 n=8). **E,** Lung cells were stained with anti-lineage markers (Lin), anti-CD90.2, ant-T-bet, anti-GATA3, and anti-RORγt antibodies. ILCs were defined as $Lin^{-}CD90.2^{+}$ cells. Representative results are shown. **F,** The numbers of total ILCs, $T\text{-}bet^{+}$ILCs, and $ROR\gamma t^{+}$ILCs were increased in the ZyA-HS3 lung. **G,** Lung cells gated on ILCs were stained for GM-CSF, T-bet, and RORγt. **H,** The numbers of $GM\text{-}CSF^{+}$ILCs, $GM\text{-}CSF^{+}T\text{-}bet^{+}$ILCs, and $GM\text{-}CSF^{+}ROR\gamma t^{+}$ILCs were increased in the ZyA-HS2,3 lungs (SAL n=5,

ZyA-HS2 and HS3 n=8). Data are shown as mean ± SEM. *, P < 0.05; **, P < 0.01; ***, P < 0.001, Student's t tests (**A**), Kruskal-Wallis tests (**B, F**), Mann-Whitney U-tests (**D, H**).

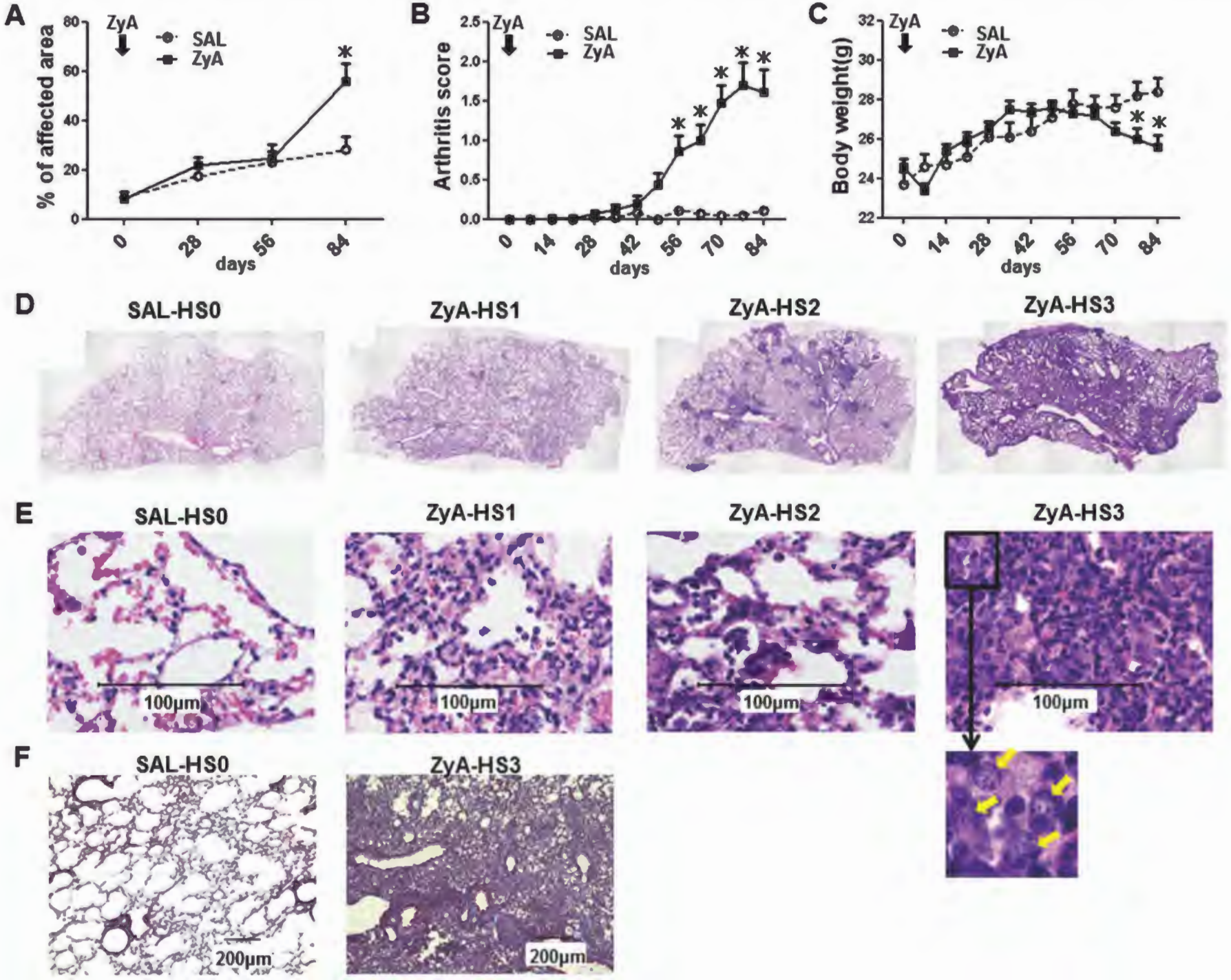
Figure 4. CD11b^{+}Gr1^{dim} cells were differentiated from M-MDSCs with GM-CSF and IL4 stimulation in vitro. **A, B,** GM-CSF stimulation induced the differentiation of CD11b^{+}Gr1^{dim} cells from total lung cells, facilitated by IL-4 stimulation. Most of the in-vitro-generated CD11b^{+}Gr1^{dim} cells expressed CD11c (Control n=5, GM-CSF n=5, GM-CSF+IL-4 n=5). Representative results are shown in **A**. **C,** Microscopic examination and flow cytometric analysis based on FSC and SSC parameters of in-vitro-generated CD11b^{+}Gr1^{dim} cells; these cells were larger than lymphocytes. **D,** Microscopic examination, H&E staining, and flow cytometric analysis based on FSC and SSC parameters of CD11b^{+}Gr1^{dim} cells from the ZyA-HS3 lung. The large cells with bright cytoplasm were found only in the ZyA-HS3 lung. Flow cytometry showed that the CD11b^{+}Gr1^{dim} cells were larger than the CD11b^{+}Gr1^{+} cells. **E, F,** CD11b^{+}Ly6C^{high} cells (M-MDSCs) were isolated from total lung cells by FACS sorting (**E**, upper). Stimulating the CD11b^{+}Ly6C^{high} cells with GM-CSF (and IL-4) induced their differentiation into CD11b^{+}Gr1^{dim} cells (**E**, lower panel, and **F**) (Control n=4, GM-CSF n=3, GM-CSF+IL-4 n=4). Data are shown as mean ± SEM. *, P < 0.05; **, P < 0.01; *** , P < 0.001, Mann-Whitney U-tests.

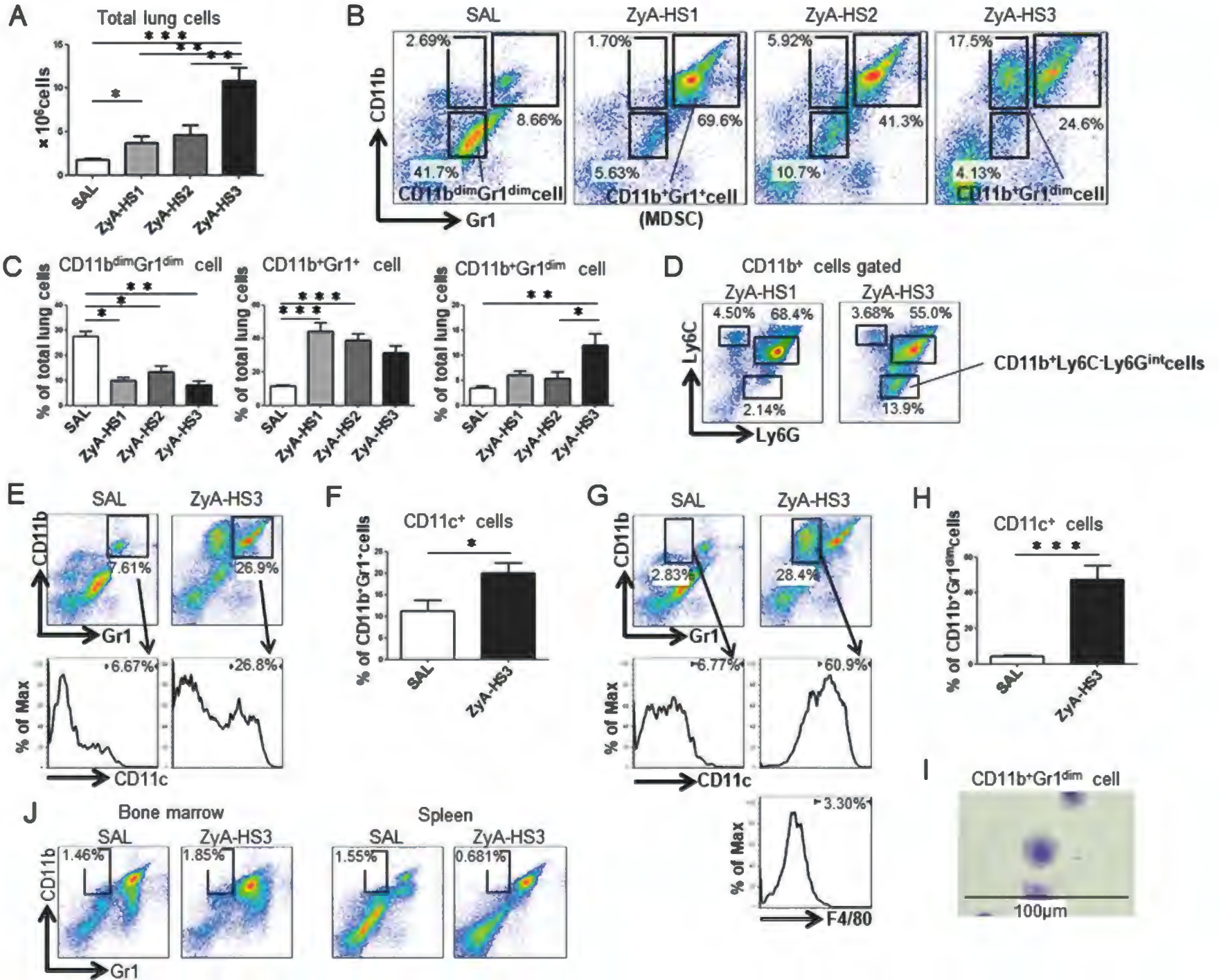
Figure 5. CD11b^{+}Gr1^{dim} cells were tolDC-like cells with immunosuppressive characteristics. **A,** CSFE-labeled naïve CD4^{+} cells were cultured alone or in a

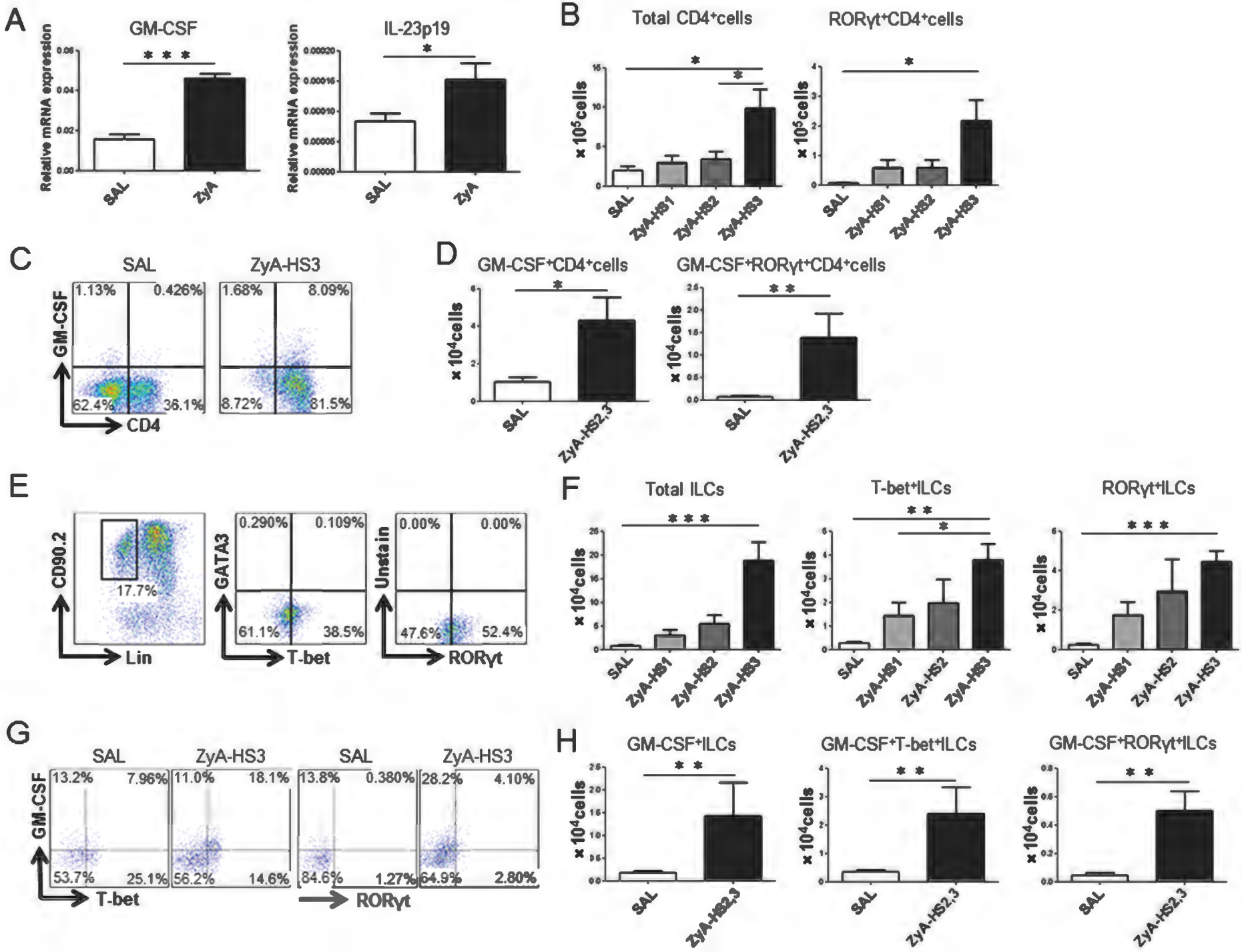
1:1 ratio with lung-MDSCs, $CD11b^{+}Gr1^{dim}$ cells, or BM-MDSCs from ZyA-HS3 mice, and were stimulated with anti-CD3 and anti-CD28 monoclonal antibodies. $CD11b^{+}Gr1^{dim}$ cells, lung-MDSCs, and BM-MDSCs suppressed T-cell proliferation. **B,** PD-L1 levels in lung-MDSCs and $CD11b^{+}Gr1^{dim}$ cells; Representative results are shown. **C,** PD-L1 was elevated in MDSCs and $CD11b^{+}Gr1^{dim}$ cells from ZyA-HS3 lungs. **D, E,** CD80 was elevated in $CD11b^{+}Gr1^{dim}$ cells from ZyA-HS3 lungs. MDSCs in SAL-treated and ZyA-HS3 lungs expressed CD80 at comparable levels. **F,** In-vitro-generated $CD11b^{+}Gr1^{dim}$ cells suppressed T-cell proliferation; in contrast, in-vitro-generated BMDCs facilitated it. **G,** PD-L1 was expressed more strongly by in-vitro-generated $CD11b^{+}Gr1^{dim}$ cells than by in-vitro-generated BMDCs; the CD80 expression was similar between these cells. **H,** The concentrations of TGF-β1 in culture supernatant were measured by an enzyme-linked immunosorbent assay. **I,** The addition of anti-TGF-β Ab (αTGF) while generating $CD11b^{+}Gr1^{dim}$tolDC-LCs partially reduced their suppressive function on T cell proliferation. Data are shown as mean ± SEM. *, $P < 0.05$; **, $P < 0.01$; ***, $P < 0.001$, Kruskal-Wallis tests (**C, E**), Student's t tests (**H**).

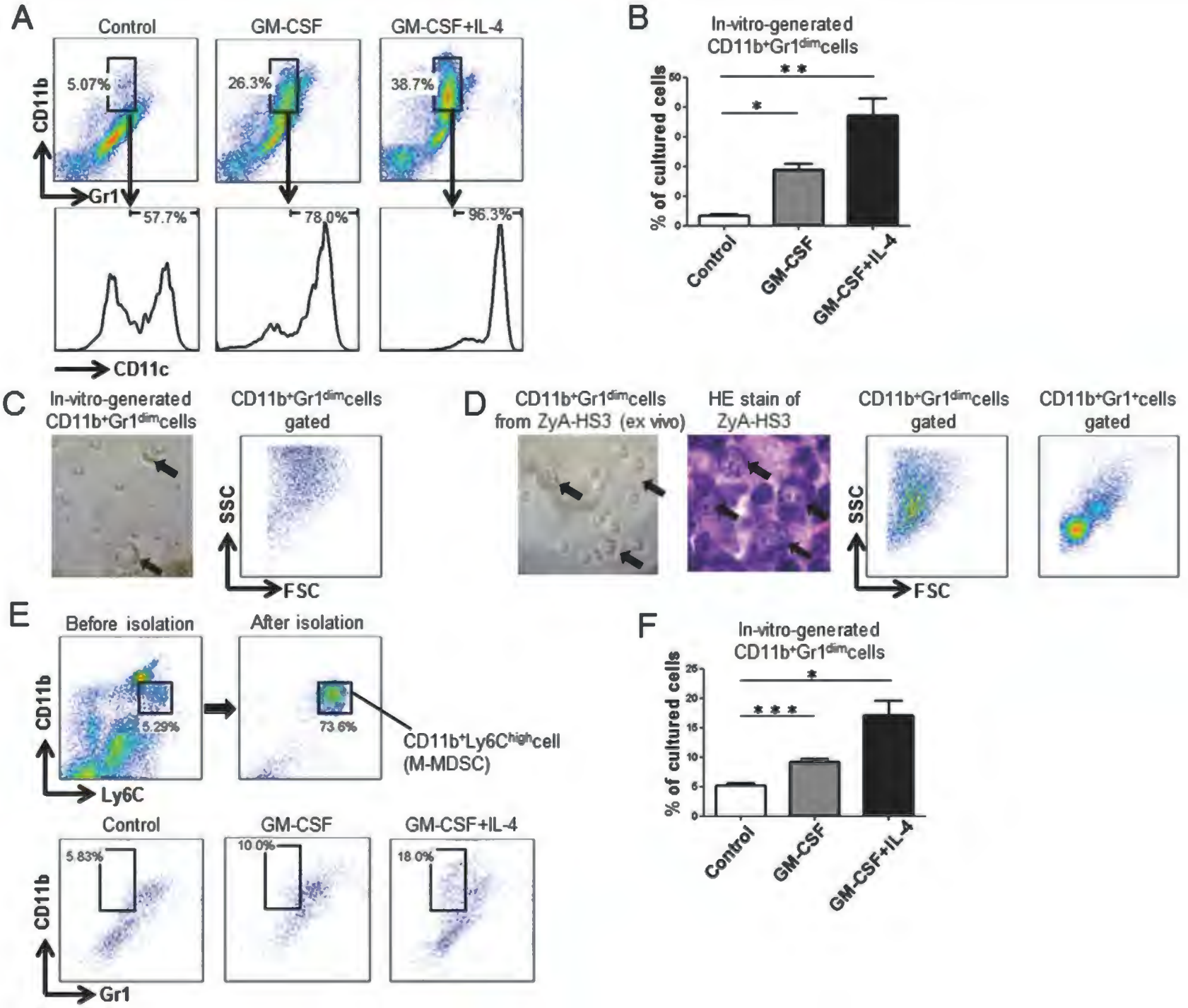
Figure 6. Adoptive transfer of in-vitro-generated $CD11b^{+}Gr1^{dim}$tolDC-LCs suppressed the progression of ILD in ZyA-treated SKG mice. **A,** Isolation of in-vitro-generated $CD11b^{+}Gr1^{dim}$tolDC-LCs. **B,** Adoptive transfer protocol. In-vitro-generated $CD11b^{+}Gr1^{dim}$tolDC-LCs (5×10^{5} cells) were adoptively transferred into the ZyA-treated SKG mice (n=6) every two weeks for three months. Normal saline was injected as a control (n=10). **C,** Representative histological results

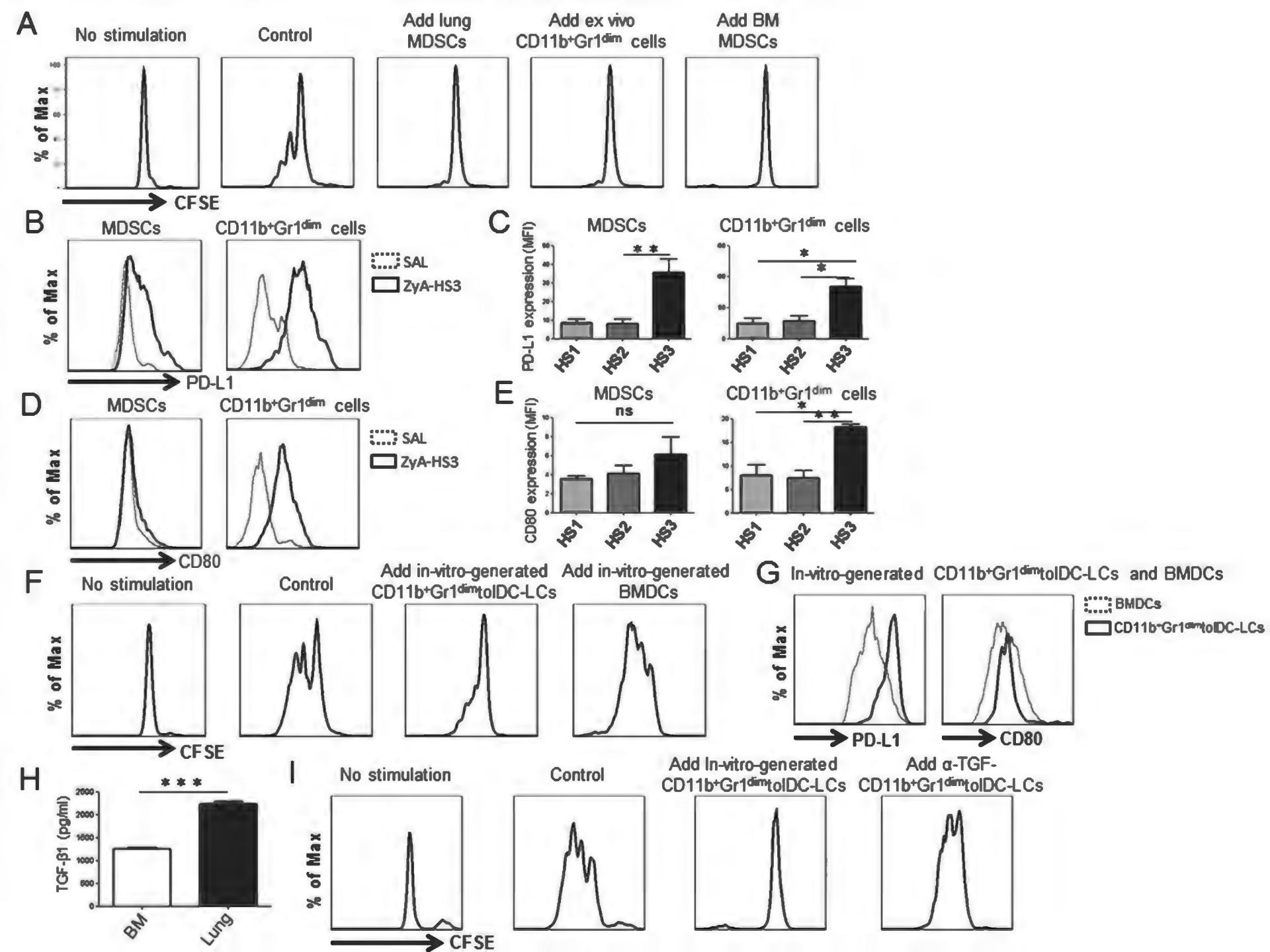
from the lungs of $CD11b^{+}Gr1^{dim}$tolDC-LCs-transferred and control mice are shown. **D,** The percentage of affected area in the lung of in-vitro-generated $CD11b^{+}Gr1^{dim}$tolDC-LCs-transferred and that of control mice. Data are shown as mean ± SEM. *, $P < 0.05$, Student's t tests (**D**).


A
% of affected area
ZyA
SAL
ZyA
days
B
Arthritis score
ZyA
SAL
ZyA
days
C
Body weight(g)
ZyA
SAL
ZyA
days
D
SAL-HS0
ZyA-HS1
ZyA-HS2
ZyA-HS3
E
SAL-HS0
ZyA-HS1
ZyA-HS2
ZyA-HS3
100μm
F
SAL-HS0
ZyA-HS3
200μm


A
Total lung cells
× 10⁶cells
SAL
ZyA-HS1
ZyA-HS2
ZyA-HS3
B
SAL
ZyA-HS1
ZyA-HS2
ZyA-HS3
CD11b
Gr1
2.69%
8.66%
41.7%
CD11b^dimGr1^dimcell
1.70%
69.6%
5.63%
CD11b⁺Gr1⁺cell
(MDSC)
5.92%
41.3%
10.7%
17.5%
24.6%
4.13%
CD11b⁺Gr1^dimcell
C
CD11b^dimGr1^dim cell
CD11b⁺Gr1⁺ cell
CD11b⁺Gr1^dim cell
% of total lung cells
D
CD11b⁺ cells gated
ZyA-HS1
ZyA-HS3
Ly6C
Ly6G
4.50%
68.4%
2.14%
3.68%
55.0%
13.9%
CD11b⁺Ly6C⁻Ly6G^intcells
E
SAL
ZyA-HS3
CD11b
Gr1
7.61%
26.9%
% of Max
6.67%
26.8%
CD11c
F
CD11c⁺ cells
% of CD11b⁺Gr1⁺cells
G
SAL
ZyA-HS3
CD11b
Gr1
2.83%
28.4%
% of Max
6.77%
60.9%
CD11c
3.30%
F4/80
H
CD11c⁺ cells
% of CD11b⁺Gr1^dimcells
I
CD11b⁺Gr1^dim cell
100μm
J
Bone marrow
Spleen
SAL
ZyA-HS3
CD11b
Gr1
1.46%
1.85%
1.55%
0.681%

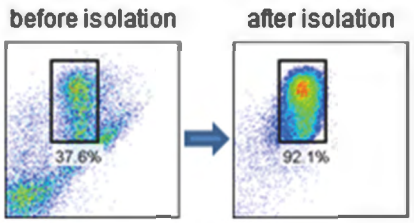

A
GM-CSF
IL-23p19
Relative mRNA expression
SAL
ZyA
B
Total CD4+cells
RORγt+CD4+cells
× 10^5cells
SAL
ZyA-HS1
ZyA-HS2
ZyA-HS3
C
SAL
ZyA-HS3
GM-CSF
CD4
1.13%
0.426%
62.4%
36.1%
1.68%
8.09%
8.72%
81.5%
D
GM-CSF+CD4+cells
GM-CSF+RORγt+CD4+cells
× 10^4cells
SAL
ZyA-HS2,3
E
CD90.2
Lin
17.7%
GATA3
T-bet
0.290%
0.109%
61.1%
38.5%
Unstain
RORγt
0.00%
0.00%
47.6%
52.4%
F
Total ILCs
T-bet+ILCs
RORγt+ILCs
× 10^4cells
G
SAL
ZyA-HS3
SAL
ZyA-HS3
GM-CSF
T-bet
RORγt
13.2%
7.96%
53.7%
25.1%
11.0%
18.1%
56.2%
14.6%
13.8%
0.380%
84.6%
1.27%
28.2%
4.10%
64.9%
2.80%
H
GM-CSF+ILCs
GM-CSF+T-bet+ILCs
GM-CSF+RORγt+ILCs
× 10^4cells
SAL
ZyA-HS2,3


A
Control
GM-CSF
GM-CSF+IL-4
CD11b
Gr1
5.07%
26.3%
38.7%
57.7%
78.0%
96.3%
CD11c
B
In-vitro-generated
CD11b+Gr1dimcells
% of cultured cells
Control
GM-CSF
GM-CSF+IL-4
C
In-vitro-generated
CD11b+Gr1dimcells
CD11b+Gr1dimcells
gated
SSC
FSC
D
CD11b+Gr1dimcells
from ZyA-HS3 (ex vivo)
HE stain of
ZyA-HS3
CD11b+Gr1dimcells
gated
CD11b+Gr1+cells
gated
SSC
FSC
E
Before isolation
After isolation
CD11b
Ly6C
5.29%
73.6%
CD11b+Ly6Chighcell
(M-MDSC)
Control
GM-CSF
GM-CSF+IL-4
5.83%
10.0%
18.0%
CD11b
Gr1
F
In-vitro-generated
CD11b+Gr1dimcells
% of cultured cells
Control
GM-CSF
GM-CSF+IL-4

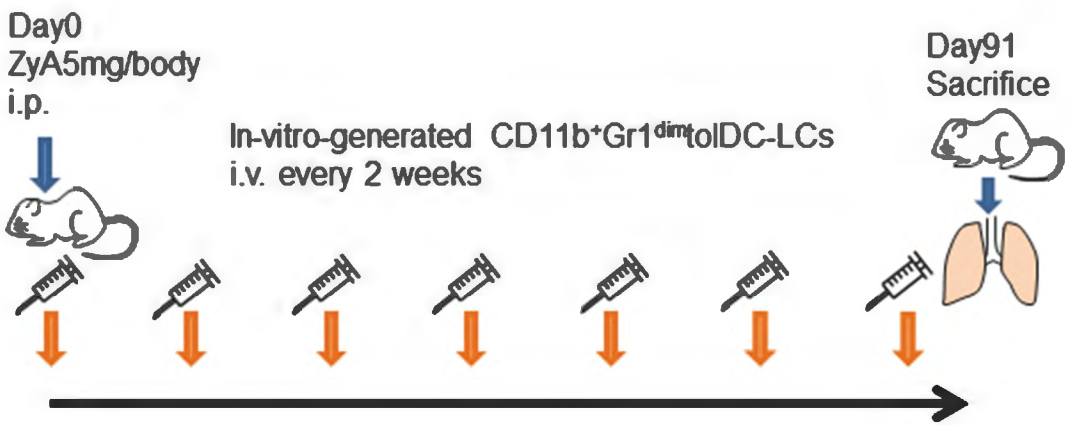

A
No stimulation
Control
Add lung MDSCs
Add ex vivo CD11b+Gr1dim cells
Add BM MDSCs
% of Max
CFSE
B
MDSCs
CD11b+Gr1dim cells
SAL
ZyA-HS3
% of Max
PD-L1
C
MDSCs
CD11b+Gr1dim cells
PD-L1 expression (MFI)
HS1
HS2
HS3
D
MDSCs
CD11b+Gr1dim cells
SAL
ZyA-HS3
% of Max
CD80
E
MDSCs
CD11b+Gr1dim cells
ns
CD80 expression (MFI)
HS1
HS2
HS3
F
No stimulation
Control
Add in-vitro-generated CD11b+Gr1dimtolDC-LCs
Add in-vitro-generated BMDCs
% of Max
CFSE
G
In-vitro-generated CD11b+Gr1dimtolDC-LCs and BMDCs
BMDCs
CD11b+Gr1dimtolDC-LCs
% of Max
PD-L1
CD80
H
TGF-β1 (pg/ml)
BM
Lung
I
No stimulation
Control
Add In-vitro-generated CD11b+Gr1dimtolDC-LCs
Add α-TGF-CD11b+Gr1dimtolDC-LCs
% of Max
CFSE

A

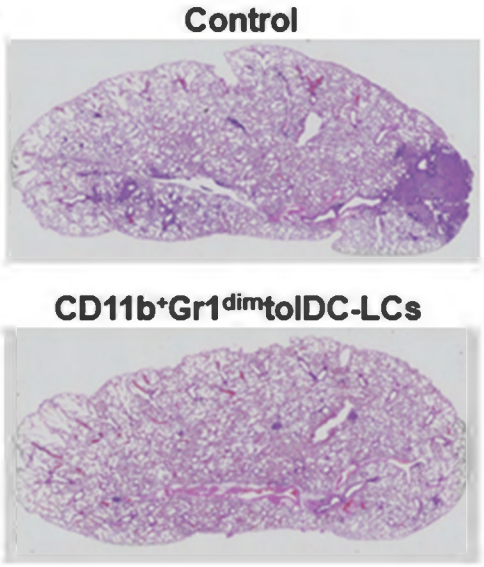
In-vitro-generated
CD11b^{+}Gr1^{dim}tolDC-LCs



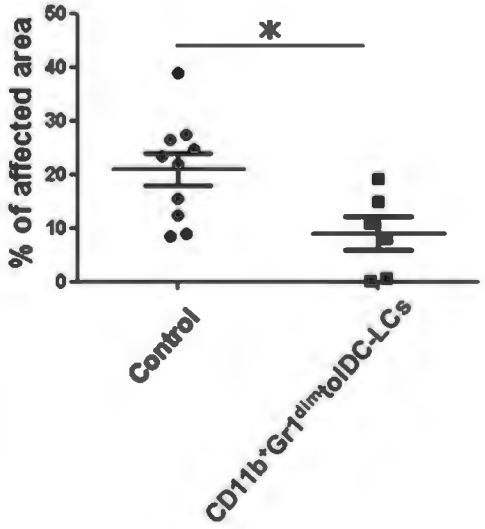
B

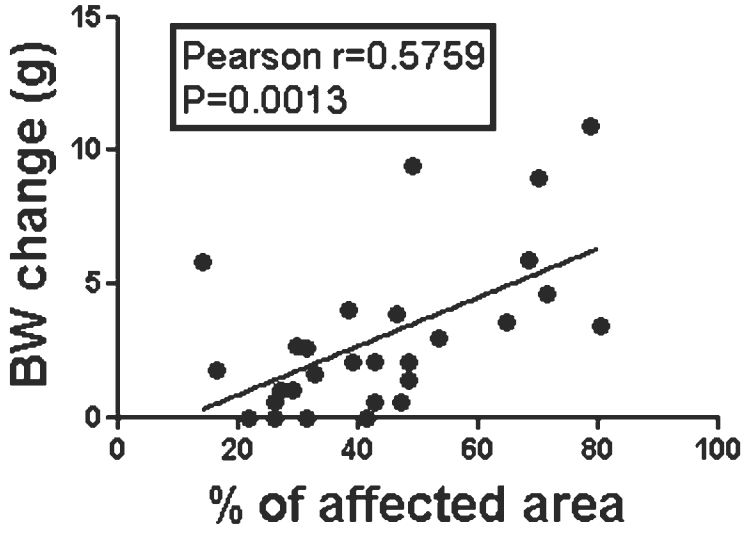


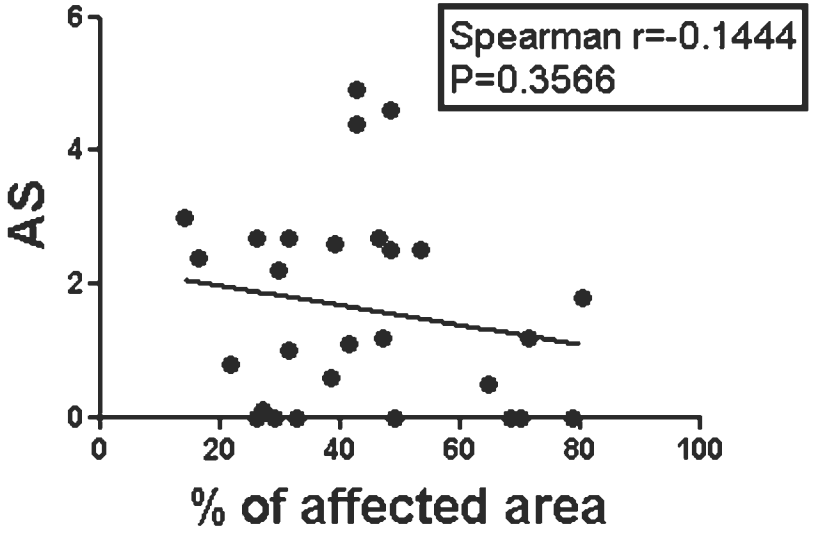
C

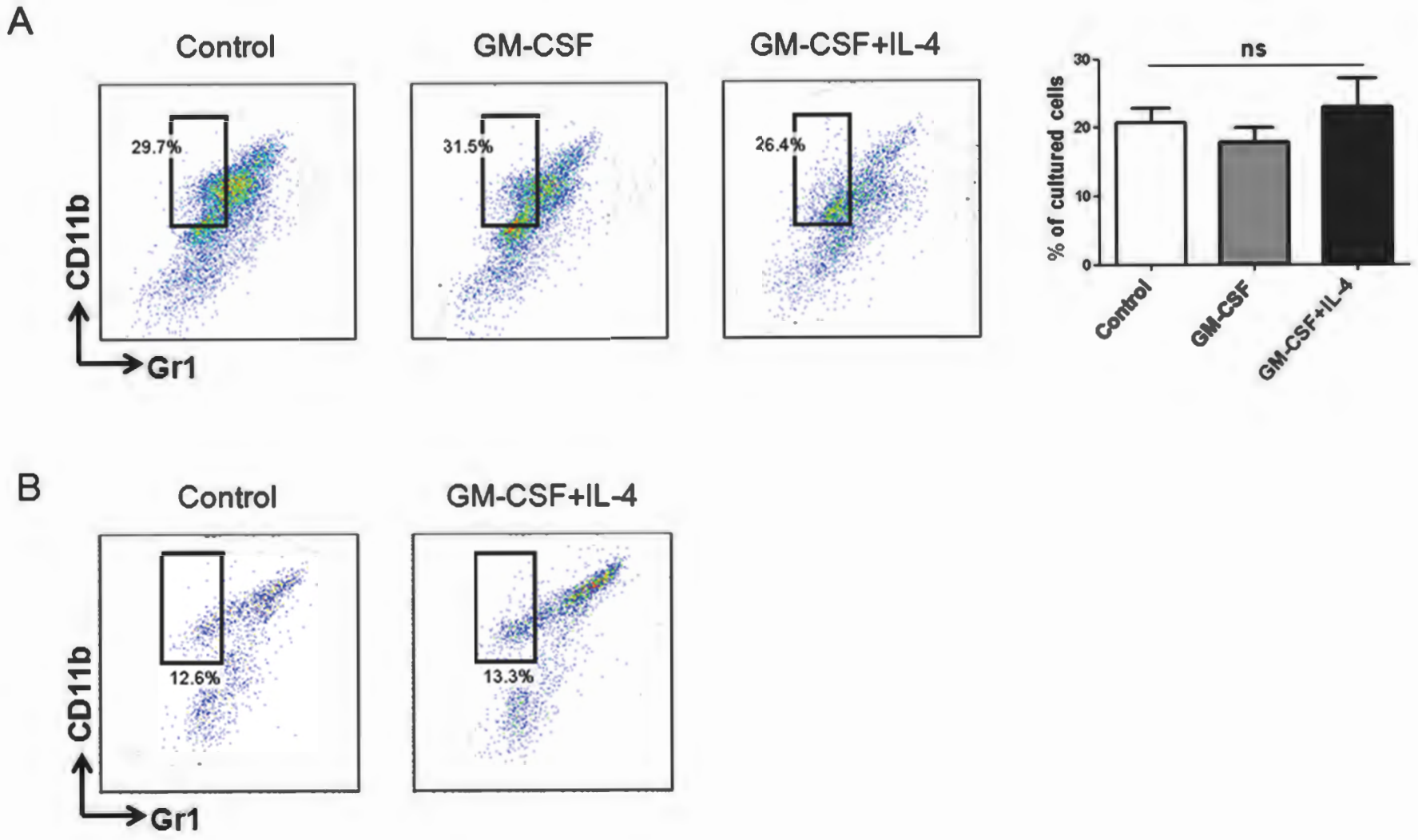


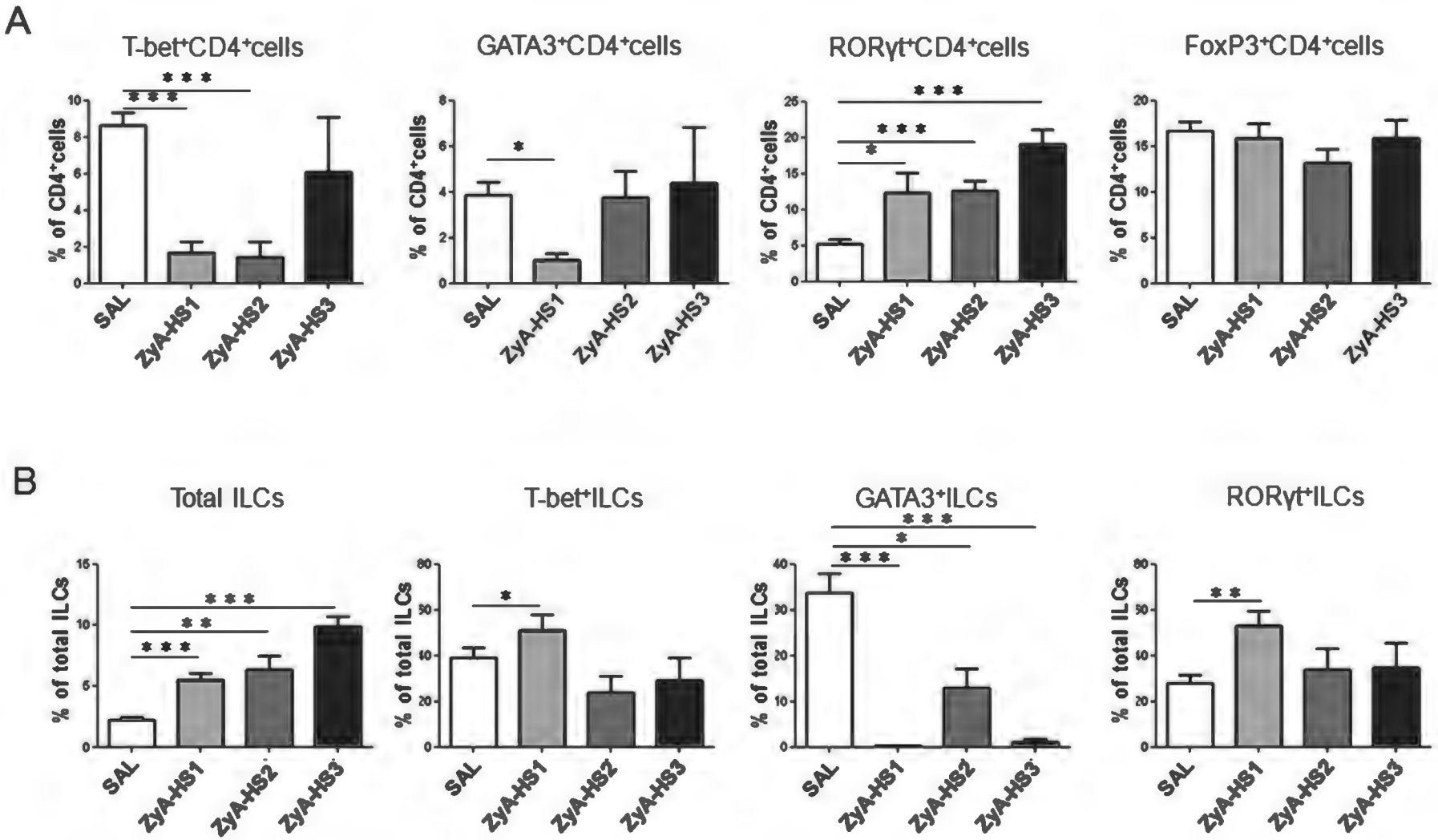
D




Pearson r=0.5759
P=0.0013
BW change (g)
% of affected area
0
5
10
15
0
20
40
60
80
100


Spearman r=-0.1444
P=0.3566
AS
% of affected area
0
2
4
6
0
20
40
60
80
100


A
Control
GM-CSF
GM-CSF+IL-4
29.7%
31.5%
26.4%
CD11b
Gr1
ns
% of cultured cells
30
20
10
0
Control
GM-CSF
GM-CSF+IL-4
B
Control
GM-CSF+IL-4
12.6%
13.3%
CD11b
Gr1


A
T-bet+CD4+cells
GATA3+CD4+cells
RORγt+CD4+cells
FoxP3+CD4+cells
% of CD4+cells
SAL
ZyA-HS1
ZyA-HS2
ZyA-HS3
B
Total ILCs
T-bet+ILCs
GATA3+ILCs
RORγt+ILCs
% of total ILCs